

See discussions, stats, and author profiles for this publication at: <https://www.researchgate.net/publication/308606327>

# Beauty is more than skin deep: A non-invasive protocol for in vivo anatomical study using micro-CT

Article in *Methods in Ecology and Evolution* · September 2016

DOI: 10.1111/2041-210X.12661

CITATIONS

4

READS

205

5 authors, including:



**Chris Broeckhoven**

University of Antwerp

27 PUBLICATIONS 50 CITATIONS

SEE PROFILE



**Anton Du Plessis**

Stellenbosch University

109 PUBLICATIONS 327 CITATIONS

SEE PROFILE



**Cang Hui**

Stellenbosch University

267 PUBLICATIONS 2,739 CITATIONS

SEE PROFILE

Some of the authors of this publication are also working on these related projects:



Mechanical Properties of High Performance Concrete with Superabsorbent Polymers (SAP) [View project](#)



Functional morphology and evolution of osteoderms [View project](#)

All content following this page was uploaded by [Cang Hui](#) on 28 September 2017.

The user has requested enhancement of the downloaded file.

# Beauty is more than skin deep: a non-invasive protocol for *in vivo* anatomical study using micro-CT

Chris Broeckhoven<sup>1,2\*</sup>, Anton du Plessis<sup>3</sup>, Stephan Gerhard le Roux<sup>3</sup>,  
Pieter le Fras Nortier Mouton<sup>1</sup> and Cang Hui<sup>2,4</sup>

<sup>1</sup>Department of Botany & Zoology, Stellenbosch University, Private Bag X1, Matieland 7602, Stellenbosch, South Africa;

<sup>2</sup>Theoretical Ecology Group, Department of Mathematical Sciences, Stellenbosch University, Private Bag X1, Matieland 7602, Stellenbosch, South Africa; <sup>3</sup>CT Scanner Facility, Central Analytical Facilities, Stellenbosch University, Matieland 7602, Stellenbosch, South Africa; and <sup>4</sup>Theoretical and Physical Biosciences, African Institute for Mathematical Sciences, Cape Town 7945, South Africa

## Summary

1. Microcomputed tomography ( $\mu$ CT) is a widely used tool in biomedical research, employed to investigate tissues and bone structures of small mammals *in vivo*. The application of *in vivo*  $\mu$ CT scanning in non-medical studies greatly lags behind the rapid advancements made in the biomedical field wherein the methodology has evolved to allow for longitudinal studies and eliminate the need to sacrifice the animal. Ecological and evolutionary studies often involve morphological measurements of a large sample of live animals; however, the potential of *in vivo*  $\mu$ CT imaging as a method for data acquisition has yet to be delineated.

2. Here, we describe a protocol for *in vivo*  $\mu$ CT imaging of the internal anatomy of reptiles and amphibians, commonly used study organisms in ecological and evolutionary research. We consider the skeletal and extraskelatal (i.e. osteoderms) bones of a lizard as a case study to elucidate the potential of *in vivo*  $\mu$ CT imaging. First, we explore the effects of various parameter settings on radiation dose, scan time and image quality. Secondly, we develop a protocol to immobilize and restrain study organisms during scanning without need for the administration of anaesthetics and compare the results of the *in vivo* protocol to images obtained *post-mortem*.

3. To immobilize animals, we replace the use of anaesthetics by cooling, thereby allowing the use of previously unsuitable rotating gantry  $\mu$ CT scanners that are readily available in scientific institutions. The resultant image quality of *in vivo*  $\mu$ CT scans is similar to that of *post-mortem*  $\mu$ CT scans, especially in the abdominal region. We discuss the effect of tube voltage, distance to X-ray source and metal filtration on radiation dose, and how these parameters could be altered to reduce the cumulative radiation dose while maintaining optimal image quality.

4. The proposed *in vivo*  $\mu$ CT protocol offers a new approach to acquire anatomical information for non-biomedical studies. We offer specific suggestions as to how the protocol can be employed to suit a variety of model organisms.

**Key-words:** bone, lizard, micro-CT, osteoderm, radiation dose, reptile, small animal imaging, X-ray

## Introduction

Since its introduction in the early 1980s (Elliott & Dover 1982), X-ray microcomputed tomography or micro-CT ( $\mu$ CT) has, especially recently, become an increasingly important tool in biological research. The production of digital 3D reconstructions with a resolution of  $<100\ \mu\text{m}$  that can be orientated or sliced to obtain different views of the anatomy of animals holds a great advantage over traditional methodologies, such as X-ray radiography and/or histology (Holdsworth & Thornton 2002). In its simplest application,  $\mu$ CT is preferred if a non-destructive method is warranted, for example to examine fossils or describe the morphology of species for which limited material is

available (O'Connor *et al.* 2010; Müller *et al.* 2011; Sherratt *et al.* 2015). The application of  $\mu$ CT in ecological and evolutionary studies, however, has greatly lagged behind its use in biomedical studies. In the biomedical field, *in vivo*  $\mu$ CT is employed to investigate the skeleton, vascular tree and organs of live mammals in order to obtain information on the disease status or disease progression (Ritman 2004; Campbell & Sophocleous 2014) and to generate therapeutic radiation doses for disease treatment (Graves *et al.* 2007). The study of bone architecture, in particular, has pushed the early advancement of  $\mu$ CT systems (Feldkamp *et al.* 1989; Kinney, Lane & Haupt 1995; Rügsegger, Koller & Müller 1996).

One of the main advantages of *in vivo*  $\mu$ CT imaging is that it allows for longitudinal studies, that is repeated measurements of small live animals at different time points (e.g.

\*Correspondence author. E-mail: cbroeck@sun.ac.za

during growth), without necessitating sacrifice of study subjects (Boyd *et al.* 2006; Foster & Ford 2010). Furthermore, *in vivo*  $\mu$ CT eliminates the interindividual variation often associated with cross-sectional study designs (Main, Lynch & van der Meulen 2010), thereby reducing the number of individuals required to obtain statistically meaningful data. The benefits of scanning live animals, and consequently the growing demand for inexpensive high-resolution biomedical imaging of small animals in preclinical research, have resulted in a variety of commercially available  $\mu$ CT scanners optimized for *in vivo* imaging (Schambach *et al.* 2010). Surprisingly, however, the potential of *in vivo*  $\mu$ CT as a tool in ecological and evolutionary studies has yet to be delineated. While these type of studies frequently employ  $\mu$ CT to describe the morphology of structures (e.g. Bauder *et al.* 2013), to our knowledge, none have so far approached the concept of *in vivo* scanning.

Two major barriers hinder the advancement and implementation of *in vivo*  $\mu$ CT. First, since  $\mu$ CT produces large data sets requiring intensive computational power and advanced 3D image analysis, the time required for analysis may be prohibitive for non-medical studies that typically require large sample sizes of morphological trait measurements to achieve the high statistical power required for hypothesis testing. The second hurdle is the limited research access to commercial  $\mu$ CT scanners optimized for living small animals due to availability, proximity and/or expense. The majority of the  $\mu$ CT scanners available in scientific institutions have a rotating specimen design in which the sample holder rotates inside the path of radiation during imaging acquisition. The main advantage is that the distance between sample and X-ray source is adjustable, thereby allowing higher-resolution scans on smaller specimens. However, this design is incompatible with the use of inhalation equipment required for the administration of anaesthesia. Following on from the second hurdle, the administration of anaesthesia in small animals is often problematic and requires practical (i.e. involvement of qualified personnel) and ethical considerations. Further advancement of  $\mu$ CT technology, including accelerating the computational speed, could easily bypass the first barrier, whereas the other barriers call for the development of non-invasive, inexpensive protocols for *in vivo* imaging using  $\mu$ CT.

Here, we develop a protocol that could be used for *in vivo*  $\mu$ CT scanning of reptilian and amphibian models. Reptiles and amphibians, especially lizards, have a long history of serving as model study organisms for an array of ecological and evolutionary studies (e.g. Losos, Schoener & Spiller 2004; Broeckhoven *et al.* 2016a). We illustrate the application of the proposed *in vivo* imaging protocol in a case study of skeletal and extraskelatal (i.e. osteoderms) anatomy. Micro-CT is especially well suited for this application due to the high contrast between the bone and soft organs surrounding it, which allows us to precisely examine the effects of resolution, radiation, immobilization and restraint on imaging quality. The ultimate aim of the study was to provide a reference and possible framework for future studies and to highlight some of the strengths and weaknesses of the *in vivo*  $\mu$ CT scanning method.

## Materials and methods

### EQUIPMENT SET-UP

Generally, a typical  $\mu$ CT set-up consists of an X-ray source that emits X-rays, which pass through an object and are recorded by an X-ray detector (Ritman 2004; Schambach *et al.* 2010). Two main types of  $\mu$ CT scanner design geometries can be discriminated: (i) rotating gantry in which the X-ray tube and X-ray detector rotate around a stationary sample holder and (ii) rotating specimen in which the sample holder rotates inside the path of radiation during imaging acquisition instead of the X-ray tube and detector rotating. In the latter design, the distance between sample and X-ray source is adjustable, thereby allowing higher-resolution scans on smaller specimens. Despite the advantages of the rotating specimen design, biomedical research typically makes use of a rotating gantry system because it facilitates the use of inhalation equipment during anaesthesia. In addition, the rotating gantry system allows for the animal to be mounted in a natural, horizontal position. Here, a commercial system with a rotating specimen design was used as our protocol does not require the administration of anaesthetics (see below). Micro-CT scanning was performed on a GE Phoenix v|tome|x L240 dual tube CT instrument (Phoenix X-ray; General Electric Sensing & Technologies, Wunstorf, Germany) located at the Central Analytical Facility, Stellenbosch University (du Plessis, le Roux & Guelpa 2016). The system contains two cone-beam X-ray tubes, one up to 240 kV and the other up to 180 kV, and a 2048  $\times$  2048 16-bit X-ray detector. The protocol can be applied with any typical commercially available  $\mu$ CT scanner, including Nikon Metrology (Leuven, Belgium), Bruker Instruments (Billerica, MA, USA) and Carl Zeiss Microimaging (Jena, Germany).

### STUDY SYSTEM

The examination of skeletal and extraskelatal bone (i.e. osteoderms) in the Armadillo lizard *Ouroborus cataphractus* (Boie 1828) served as an example to test the proposed *in vivo* imaging protocol. Bones, frequently measured using X-ray radiography, are important anatomical structures and highly informative in terms of ecological and evolutionary processes (e.g. Losos *et al.* 2002). The disadvantages of two-dimensional X-ray radiography include restriction to linear measurements, obscuring the detail and accuracy of 3D structural relationships due to structural superimposition and measurement error resulting from difficulties associated with mounting specimens in the same position. Osteoderms are embedded in the dermis layer of the skin, and hence they cannot be measured non-invasively in living organisms *in vivo* and consequently their description largely depends on histological techniques (i.e. serial sections of skin tissue) using preserved or deceased specimens (e.g. Broeckhoven, Diedericks & Mouton 2015). Recent studies illustrate the potential of  $\mu$ CT technology for investigating skeletal and extraskelatal bone (e.g. Greenbaum *et al.* 2012; Broeckhoven *et al.* 2016a). The advantages of  $\mu$ CT, in addition to linear or other dimensional measurements that can be made to high degree of accuracy, include the following: (i) the entire structure can be analysed in virtual sections in any orientation, in contrast to traditional sectioning which cannot be adjusted; (ii) volumetric information can be determined such as the object volume or void space; and (iii) the 3D location of structures can be investigated. A novel methodology that allows for high-resolution measurements of bones and osteoderm characteristics in live reptiles and amphibians is therefore strongly warranted: *in vivo*  $\mu$ CT could, for instance, increase sampling potential and allow for repeated measurements at different time points.

### IN VIVO SCANNING PROTOCOL

One of the main drawbacks of  $\mu$ CT imaging, compared to traditional 2D X-ray radiography, is that the prolonged scanning times (i) result in an increased radiation dose and (ii) require animals to remain immobile during the entire procedure. Given that both factors can highly influence the quality of the image data, several experiments were conducted to optimize the settings for *in vivo* imaging using  $\mu$ CT. For this purpose, preserved specimens were used to calculate the cumulative radiation dose under various scanning settings prior to the *in vivo*  $\mu$ CT scanning experiments. Following the radiation experiments, live specimens were used to test the immobilization and restraining protocol, and to assess the adequacy of *in vivo*  $\mu$ CT imaging in terms of image resolution and quality.

#### Radiation dose experiments

While rotating gantry  $\mu$ CT scanners are optimized to minimize radiation dose and scan time, and increase image quality (Holdsworth & Thornton 2002; Boone, Velazquez & Cherry 2004; Willekens *et al.* 2010), little information exists on the radiation dose produced in commercial systems that are not designed for *in vivo* animal studies. Because the exposure of animals to ionizing radiation is a major concern for  $\mu$ CT imaging, radiation dose experiments were conducted for various settings implemented in this work. The reference parameter settings were as follows: 120 kV, 180 mA, 0 mm Cu filtration, 105 mm distance to source, 1000 images, 500 ms capture time, 1 image averaged per rotation, no initial image skip. Next, each parameter was altered and the effect on dose rate, scan time and image quality was assessed. The distance between sample and detector was fixed at 600 mm. In order to provide estimates of the radiation dose rate, a calibrated digital dosimeter (isotrak DoseGUARD, Braunschweig, Germany) was used. Although we used a commercial dosimeter instead of thermoluminescent dosimeters commonly used for dose measurements, we expect the results to be comparable (Figueroa *et al.* 2008). A preserved lizard specimen was used to assess the effects of the various parameters on image quality. The position of the specimen was identical between successive acquisitions. Image quality was quantified by the signal-to-noise (S : N) ratio (Firbank *et al.* 1999). The S : N ratio was calculated as the ratio of the mean pixel intensity of a uniform region of interest (ROI) over the standard deviation of that region. Square ROIs, measuring  $\pm 0.5 \text{ mm}^3$ , were digitally extracted from femoral bone, osteoderm and background at identical positions among scans. We calculated the S : N ratio and averaged these values to obtain an overall measure of image quality. All reconstructions were conducted using system-supplied DATOS 2.0 software (General Electric Sensing & Technologies) with beam hardening correction. Images were obtained using the VGSTUDIO MAX 3.0 software (Volume Graphics GmbH, Heidelberg, Germany).

#### Immobilization and restraining of animals

Immobility can be achieved via the administration of injectable anaesthetics (predominantly intramuscular) (Mosley 2005), or via inhalation (Bertelsen *et al.* 2005; Sladky & Mans 2012). Although the use of anaesthetics in reptiles and amphibians is well documented (Longley 2008; Sladky & Mans 2012), the suggested doses are often anecdotal or extrapolated from mammals or birds (Mosley 2005). Consequently, anaesthetic toxicity due to administration of large doses can easily occur (Bennett 1991). Hoefer, Goodman & Downes (2003) proposed a more suitable alternative method to restrain small lizards (up to

100 mm snout-vent length) for radiography. The authors suggest to cool individuals for approximately 30 min by placing them in a refrigerator set at 10–15 °C to ensure that the study organisms are thermally incapacitated. Cooling of reptiles and amphibians is preferred over the administration of anaesthetics because it is more cost-effective, practical and does not cause additional stress or risks to the study organism. For the purpose of this study, we made two adjustments to the protocol proposed by Hoefer, Goodman & Downes (2003). First, due to the considerably longer scanning times, lizards were cooled to  $\pm 8$  °C. This temperature falls within the range of the critical thermal minima (CTmin) of various cordylid lizards (i.e. 6.3–10.2 °C; McConnachie, Alexander & Whiting 2007). The CTmin is considered the mean temperature at which cold narcosis is produced and locomotion prevented. It must, however, be noted that the CTmin is well above the lower lethal temperature recorded. For instance, while the CTmin of the cordylid *Pseudocordylus melanotus* is on average 10.2 °C, the lower lethal temperature ranges between –3.4 and –5.7 °C (McConnachie, Alexander & Whiting 2007). Lizards were transferred from their enclosure to a breathable cotton bag and placed in an inexpensive portable Herp Nursery II Incubator (Lucky Reptile, Waldkirch, Germany), which was located inside the CT scanning facility (kept at 20 °C) to allow for direct transfer from incubator to the  $\mu$ CT machine. The body temperature was measured at fixed intervals using an infrared thermometer (model 62 Mini; Fluke Inc., Washington, DC, USA).

To restrict movement, specimens were restrained in addition to cooling and were subsequently fixated in a vertical position (i.e. head up). First, each lizard was restrained between two Styrofoam plates (measuring 20 × 5 × 0.5 cm) and secured with paper tape. Secondly, the lizards were placed in a custom-built Styrofoam holder (measuring 25 × 10 × 10 cm) optimized for organisms not exceeding 20 cm total body length. A layer of crushed ice was placed between each side of the holder and the plates restraining the lizard. Thirdly, a thicker Styrofoam plate was used to close the holder and was secured with tape. Sufficient space was provided between the tail tip and the bottom of the sample holder to avoid contact of body parts with melted ice. Finally, the holder was placed inside a plastic box to avoid possible leakage of water from damaging the machine and mounted on a plastic PVC pipe that could be locked on the rotating sample holder of the machine. A 3D rendering of the sample holder is illustrated in Fig. 1. It must be noted that the mounting device did not alter the radiation dose rate and can be adjusted to suit specific needs.

#### Adequacy of *in vivo* $\mu$ CT imaging

The primary concern is that movement of live animals, specifically respiration, might introduce imaging artefacts (e.g. blurring) and, consequently, degrade image quality. For this purpose, a sample of five live lizards was scanned using the aforementioned *in vivo*  $\mu$ CT scanning protocol. For the first scan, the settings were as follows: 85 kV, 180 mA, 0.1 Cu filtration, 300 mm distance to source (spatial resolution = 100  $\mu$ m), 1000 images, 8.27 min scan time. For the second scan, the settings were as follows: 85 kV, 180 mA, 0.1 Cu filtration, 105 mm distance to source (spatial resolution = 35  $\mu$ m), 2000 images, 16.6 min scan time. A live X-ray video of an example of the *in vivo*  $\mu$ CT scanning procedure is presented in the Supporting Information (Video S1). We compared the image quality, both visually and by means of S : N ratio, of *in vivo* scans to *post-mortem* scans obtained from similarly sized preserved lizards. In the latter case, square ROIs measuring  $\pm 0.5 \text{ mm}^3$  were digitally extracted from humeral bone and osteoderm in the thoracic region, as well as femoral bone and osteoderm in the abdominal region of each specimen. First, paired samples *t*-tests were conducted using the *in vivo* scans to compare the S : N ratio of bone and

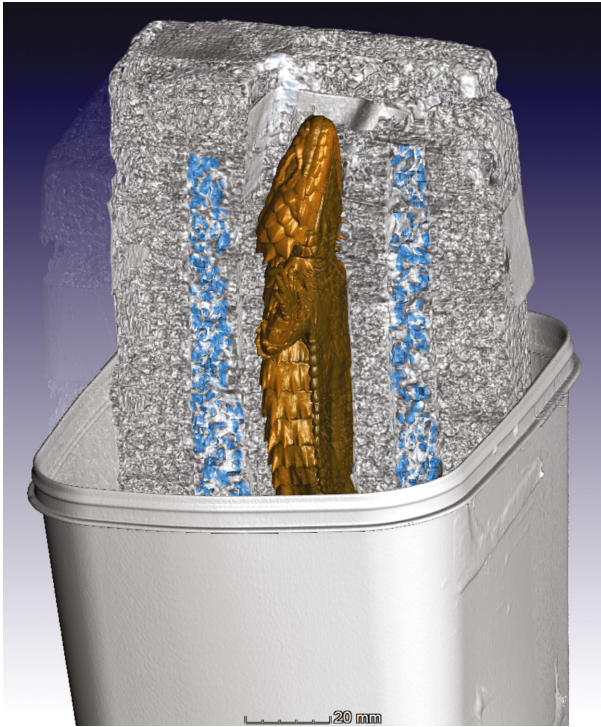


**Fig. 1.** 3D rendering of the sample holder. Cooled lizards are restrained between two thin Styrofoam plates and placed in a custom-built Styrofoam holder. A layer of crushed ice (indicated in blue) was placed between each side of the holder and the plates restraining the lizard. The holder is placed inside a plastic box to avoid leakage of water from damaging the micro-CT ( $\mu$ CT) equipment.

osteoderm between each body region and between the two scan settings. Secondly, independent samples *t*-tests were conducted to compare the S : N ratios between *in vivo* and *post-mortem* scans. All statistical analyses were conducted in SPSS STATISTICS v. 20.0.0 (SPSS Inc., Chicago, IL, USA).

#### ETHICAL NOTE

Lizards used for the study were collected in South Africa under Northern Cape Province permit number FAUNA 1541/2015. The *in vivo*  $\mu$ CT scanning protocol was approved by the Ethical Committee of Stellenbosch University (SU-ACUD15-00044). After the scanning procedure, the activity of lizards was carefully monitored for 30 days in the laboratory prior to release. In addition, we implemented a post-release monitoring period of 90 days by means of remote camera trapping (see Broeckhoven & Mouton 2015 for a full description of the set-up). No noticeable side effects of irradiation were observed in the laboratory and the majority of subjects were recovered in the field at the end of the camera trapping period. It is highly likely that all subjects survived to 90 days; however, this could not be conclusively confirmed.

## Results

#### RADIATION DOSE EXPERIMENTS

The radiation dose experiments showed that altering various scanning parameters can have major effects on

radiation dose rate, image quality and scan time (Table 1). These results are illustrated in Fig. 2. The radiation dose rate is mainly determined by the tube voltage and ranged from  $0.003 \text{ Gy min}^{-1}$  for a 50 kV scan to  $0.17 \text{ Gy min}^{-1}$  for a 120 kV scan. Hence, reducing the tube voltage from 120 to 50 kV decreased the radiation dose more than 98.5% (Fig. 2, Table 1). The second most important factor was the distance from the sample to the X-ray source. Moving the sample further away from the X-ray source decreased the radiation dose rate exponentially. The use of 1.0 mm Cu filtration lowered the radiation dose rate 65.3%, whereas the use of 0.1 or 0.5 mm Cu filtration did not significantly affect the radiation dose rate (7.9% and 18.1% reduction, respectively; Fig. 2, Table 1). Signal-to-noise ratio analyses revealed that the image quality was relatively unaffected by the scanning parameters, except for the degree of Cu filtration: image quality decreased 31.8–54.1% when Cu filtration was used (Fig. 2, Table 1). Image quality can be improved by altering the number of images averaged per rotation and/or skipping the initial image; however, these parameter adjustments greatly increase scanning duration and consequently radiation dose (Fig. 2, Table 1).

#### ADEQUACY OF *IN VIVO* $\mu$ CT IMAGING

Lizards remained near-immobile in the holder for the entire duration of the scan (i.e. 8–16 min). The S : N ratios of bone and osteoderms in the abdominal region were similar to that in the thoracic region (paired samples *t*-test, all  $P > 0.16$ ). Furthermore, the duration of the scan did not seem to influence the results because we did not detect any differences between the scan settings (paired samples *t*-test, all  $P > 0.05$ ). Likewise, the S : N ratios of bone and osteoderms did not differ significantly between *in vivo* and *post-mortem* scans (independent samples *t*-test, all  $P \geq 0.05$ ). Although the image quality of a transversal section of the thorax was almost identical to that of the abdominal region, breathing resulted laterally in a blurry thoracic region (Fig. 3).

## Discussion

The application of *in vivo*  $\mu$ CT imaging outside the biomedical field has received very little attention in the past due to the poor accessibility to  $\mu$ CT scanners optimized for small animals, in addition to the constraints of obtaining appropriate image quality, radiation dose and the practical aspect of immobilization by administering anaesthetics. Our study aimed to develop and test an inexpensive protocol that can be used to scan live reptiles and amphibians using a commercial rotating gantry  $\mu$ CT scanner without the need for anaesthetics. First, we assess the expediency of our immobilization protocol by comparing *in vivo* to *post-mortem*  $\mu$ CT imaging. Secondly, we discuss radiosensitivity in reptiles and amphibians in general. Thirdly, we explore the effects of scanning parameters on radiation dose and image quality. Finally, we present a general framework for

**Table 1.** Scan parameter settings used for the radiation dose experiment. Scan 0 is the reference scan to which all other scans are compared. The adjusted scanning parameter is indicated in bold. In addition, the scan time under the specific settings is presented, as well as the signal-to-noise (S : N) ratio which served as proxy for image quality

Scan	Scan parameters								Radiation dose (Gy)	Scan time (min)	Dose rate (Gy min <sup>-1</sup> )	S : N ratio
	kV	mA	Cu	DS	IMG	AVG	SKP	CT				
0	120	180	0	105	1000	1	0	500	1.42	8:27	0.17	40.4
A1	120	180	0	<b>225</b>	1000	1	0	500	0.35	8:27	0.04	37.4
A2	120	180	0	<b>300</b>	1000	1	0	500	0.19	8:27	0.02	35.9
B1	<b>50</b>	180	0	105	1000	1	0	500	0.02	8:27	0.003	40.7
B2	<b>85</b>	180	0	105	1000	1	0	500	0.49	8:27	0.06	43.4
C1	120	<b>100</b>	0	105	1000	1	0	500	1.26	8:27	0.15	36.4
D1	120	180	<b>0.1</b>	105	1000	1	0	500	1.31	8:27	0.16	39.1
D2	120	180	<b>0.5</b>	105	1000	1	0	500	1.12	8:27	0.14	20.6
D3	120	180	<b>1.0</b>	105	1000	1	0	500	0.49	8:27	0.06	17.2
E1	120	180	0	105	<b>500</b>	1	0	500	0.70	4:07	0.17	34.0
E2	120	180	0	105	<b>2000</b>	1	0	500	2.86	16:6	0.17	45.7
F1	120	180	0	105	1000	<b>2</b>	0	500	2.86	16:6	0.17	43.4
F2	120	180	0	105	1000	<b>3</b>	0	500	4.28	24:8	0.17	47.8
G1	120	180	0	105	1000	1	<b>1</b>	500	2.86	16:6	0.17	40.3
H1	120	180	0	105	1000	<b>2</b>	<b>1</b>	500	4.28	24:8	0.17	46.0
I1	120	180	0	105	1000	1	0	<b>250</b>	1.36	7:91	0.17	39.4
I2	120	180	0	105	1000	1	0	<b>131</b>	1.09	6:33	0.17	28.3

DS, distance to X-ray source; IMG, number of images; AVG, number of images averaged per rotation; SKP, skip of first image; CT, capture time.

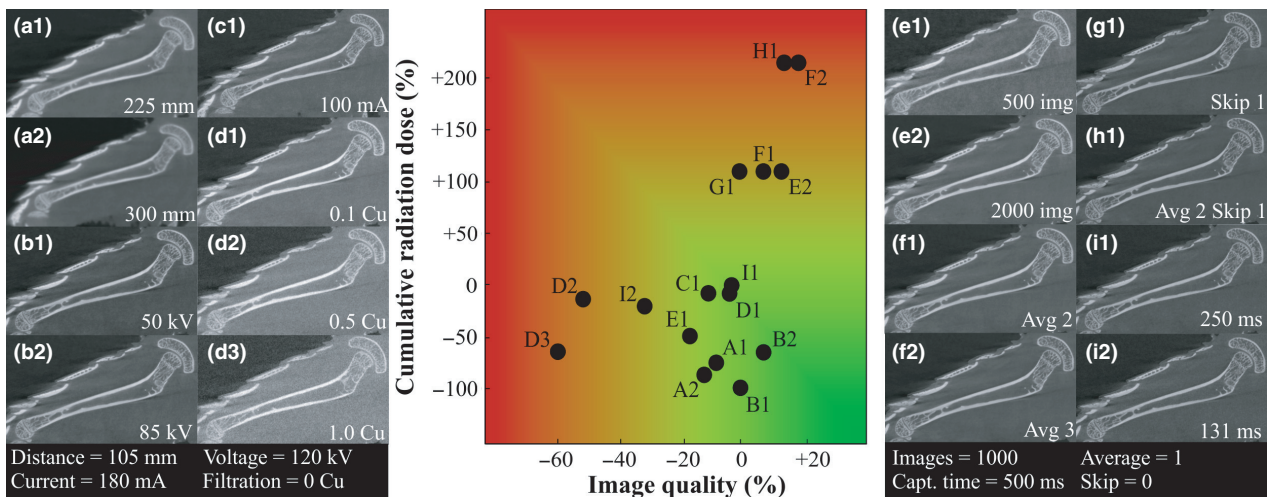


**Fig. 2.** Image depicting the effects of various parameter settings (a–i) on the cumulative radiation dose and image quality. The black circles show the increase (or decrease) in cumulative radiation dose and image quality for each parameter adjustment (indicated in the bottom right corner of each image) relative to the reference parameter setting (indicated in the black box). The colour gradient represents the strength of the adjustment effect, from green (positive: radiation reduction and/or increase in image quality) to red (negative: high radiation dose and/or reduction in image quality). In addition, a transversal section of the hind leg illustrating the image quality is presented for each parameter adjustment. The graph summarizes the results presented in Table 1.

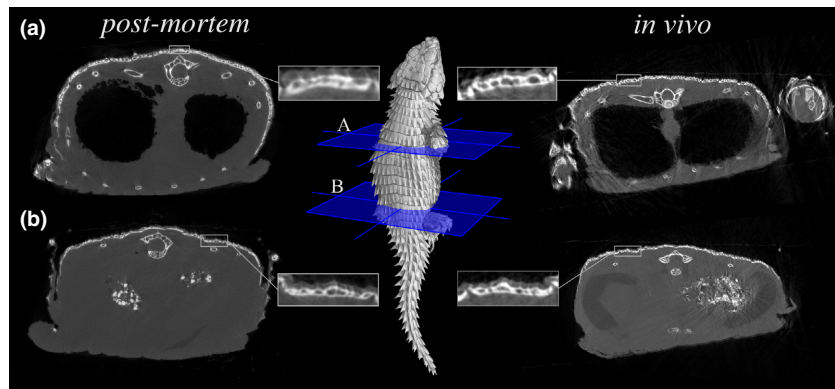
*in vivo*  $\mu$ CT scanning in reptiles and amphibians based on our findings.

#### IN VIVO VS. POST-MORTEM $\mu$ CT IMAGING

The most relevant factor that discriminates *in vivo* from *post-mortem*  $\mu$ CT imaging relates to animal manipulation since small animals are always anaesthetized during *in vivo* imaging studies (e.g. Kagadis *et al.* 2010). In the case of commercial  $\mu$ CT scanners with a rotating specimen design, the

administration of inhalation anaesthetics is complicated by the fact that the inhalation apparatus may conflict with the sample rotation. Our results show that, by taking advantage of the poikilothermic nature of reptiles, *in vivo* scanning can be successfully accomplished without the administration of anaesthetics. The image quality of *in vivo* scans is similar to those of *post-mortem* scans even for the thorax region (Table 1). It must, however, be noted that the S : N ratio may not be the perfect measure of the image quality, since various factors including edge sharpness or motion blur are not considered in

**Fig. 3.** Visual comparison of image quality between *in vivo* and *post-mortem* scans at 35  $\mu$ m spatial resolution (i.e. 105 mm distance to X-ray source). Transversal sections through the thoracic and abdominal region (a and b) show that correct immobilization during *in vivo* micro-CT ( $\mu$ CT) scanning produces images of comparable quality to those obtained *post-mortem*. The lateral sides of the thoracic region are, however, clearly blurred as a result of the breathing. Hence, analysis of anatomical features in this region might be problematic.



this measurement. The lateral sides of the specimen in the thoracic region are clearly blurred as a result of the breathing. This may affect dimensional measurements and the ability to discriminate between smaller structures in the thoracic region. Direct measurement methods of edge sharpness or image sharpness over the whole image are therefore important and require future development.

Correct immobilization is pivotal to ensure that no movement besides breathing occurs during the scanning procedure, thereby eliminating unnecessarily repetitive scanning. In order to achieve correct immobilization, two factors have to be taken into consideration: cooling rate and CTmin. The cooling rate of poikilotherms is predominantly determined by body mass and generally ranges from 0.5 to 1.5  $^{\circ}\text{C min}^{-1}$  in small reptiles and amphibians (Kour & Hutchison 1970; Claussen & Art 1981). Larger lizards and crocodiles have cooling rates of 0.1–0.5  $^{\circ}\text{C min}^{-1}$  (Bartholomew & Tucker 1964; Bartholomew & Lasiewski 1965; Bartholomew, Tucker & Lee 1965; Grigg & Alchin 1976; Smith 1976) and might require a substantial increase in cooling time. Cooling rates of turtles (i.e.  $<0.2$   $^{\circ}\text{C min}^{-1}$ ) appear to be considerably lower than those of similarly sized reptiles (Weathers & White 1971; Spray & May 1972). Likewise, the cooling rate of 0.2  $^{\circ}\text{C min}^{-1}$  observed in *O. cataphractus* during the study was considerable lower than expected for similarly sized lizards. The thermoregulatory role of dermal bone, such as osteoderms, and carapaces has been proposed by various authors (Seidel 1979; Sturbaum 1982; Broeckhoven, Diedericks & Mouton 2015) and must be taken into account during the experimental design of the immobilization phase. The second factor that plays an important role during cooling is the determination of the CTmin of the study organism. Critical thermal minima for reptiles and amphibians usually range between 1 and 10  $^{\circ}\text{C}$  (McConnachie, Alexander & Whiting 2007). Temperate species, or those that occur at high altitude, often have a lower CTmin, whereas the CTmin of (sub)tropical species approximates the higher end (John-Alder, Morin & Lawler 1988). We suggest that species-specific cooling rates and CTmin data should be obtained from literature or, if absent, extrapolated from closely related taxa. The references presented here are by no means complete, but can be used as a guideline. Similar to cooling rates, the heating rate of poikilotherms relates to body mass (Bartholomew & Tucker 1964; Claussen & Art 1981). However, the temperature within

the sample holder remained constant throughout the image acquisition and immobilization of study subjects is therefore unlikely to be affected by heating rate.

#### RADIOSENSITIVITY IN REPTILES AND AMPHIBIANS

The most important consideration for the development of an *in vivo*  $\mu$ CT imaging protocol (besides proper immobilization) is the potential negative effects of irradiation. Remarkably, little to no research has been conducted on this topic in amphibians and reptiles during the last 40 years (reviewed in Table 2). Radiosensitivity is determined by the lethal dose,  $\text{LD}_{50(x)}$ , that is the cumulative radiation dose that will kill 50% of the study organisms over a time period 'x' (expressed in days). Sterility (Altland, Highman & Wood 1951; Turner *et al.* 1967; Turner & Medica 1977; Pearson *et al.* 1978; Nagy & Medica 1985; but see Brooks 1962), hematopoietic depression (Cosgrove 1965; Bair, Park & Clarke 1968; Conger & Clinton 1973; Kleinbergs-Krisans & Catlett 1975) and necrosis of the epithelium especially in amphibians (Brunst 1958; Lappenbusch & Willis 1970) have been repeatedly reported at  $\text{LD}_{50(30)}$ . Yet, most of our current knowledge on the effects of irradiation on the body during  $\mu$ CT is inferred from medical studies conducted on laboratory mammals (e.g. Carlson *et al.* 2007; Detombe *et al.* 2013; Vande Velde *et al.* 2015). The average radiation dose during medical  $\mu$ CT studies on mice falls in the range of 0.02–0.96 Gy (Table 3), far below their  $\text{LD}_{50(30)}$  of 5–7.6 Gy (Taschereau, Chow & Chatziioannou 2006). At these doses,  $\mu$ CT image acquisition does not appear to result in DNA, cell or tissue damage in mice (Brouwers, Van Rietbergen & Huiskes 2007; Klinck, Campbell & Boyd 2008; Beck *et al.* 2013). Although caution is required when high radiation doses are being used (Vande Velde *et al.* 2015), a cumulative radiation dose of  $\approx 5$  Gy appears to have no significant negative effects on tissues in mice (Detombe *et al.* 2013). The  $\text{LD}_{50(30)}$  in reptiles and amphibians ranges from 10 to 45 Gy in lizards, frogs and salamanders to 80 Gy in turtles (Table 2). It would be tempting to assume that these poikilothermic organisms have a higher radioresistance compared to mammals; however, several authors have suggested that the high  $\text{LD}_{50(30)}$  of amphibians and reptiles is merely a consequence

of long latency periods (Tester, Ewert & Siniff 1970). Studies that assess survival clearly show that longer test periods greatly reduce the LD<sub>50</sub>. For instance, the LD<sub>50(30)</sub> for the common box turtle (*Terrapene carolina*) is 80 Gy, while the LD<sub>50(120)</sub> for the same species is 12.5 Gy (Altland, Highman & Wood 1951). Although similar patterns have been observed in other reptiles and amphibians (e.g. DiVita & Barr 1963; Kleinbergs-Krisans & Catlett 1975), the effect

seems to be more prominent in reptiles than in amphibians (Table 2).

Organismal radiosensitivity might be affected by other factors as well. First, the temperature at which the study subject is maintained during and after irradiation could have a prominent effect on radiosensitivity in poikilothermic organisms. Low temperatures during irradiation tend to decrease radiosensitivity (Storer & Hempelmann 1952; Belli & Bonte

**Table 2.** Summary of studies examining radiosensitivity (LD<sub>50</sub>) in reptiles and amphibians. The assessment time (in days) is indicated in brackets. For the studies that make use of X-rays, the scanning parameters, including voltage (kV), current (mA) and thickness of filters (in mm), are indicated. In addition, the radiation dose rate (Gy min<sup>-1</sup>) is given for all studies

Taxa	kV	mA	Filter Cu/Al	Dose rate	LD <sub>50</sub>	References
<b>Squamata</b>						
<i>Uta stansburiana</i>	Co-60			2.0	16.9 (30)	Turner <i>et al.</i> (1967)
	Co-60			1.0	22.1 (30)	Turner <i>et al.</i> (1967)
	Co-60			1.0	21.0 (30)	Turner <i>et al.</i> (1967)
	280	20	0/0	0.7	11.0 (30)	Dana & Tinkle (1965)
	250	20	0/0			
<i>Lygosoma laterale</i>	Co-60			1.0	>15.0 (-)	Brooks (1962)
<i>Sceloporus occidentalis</i>	300	na	na	na	15.0 (30)	Willis & McCourry (1968)
	Co-60					
<i>Chalcides ocellatus</i>	Co-60			60	12.5 (30)	Roushdy <i>et al.</i> (1979)
<i>Uma notata</i>	250	15	0.5/1	1.1	240 (30)	Kleinbergs-Krisans & Catlett (1975)
	250	15	0.5/1	1.1	30.0 (60)	Kleinbergs-Krisans & Catlett (1975)
<i>Calotes versicolor</i>	Co-60			9.0	45.0 (30)	Kothari & Patil (1975)
<i>Anolis carolinensis</i>	300	20	0/0.1 + 3	1.2	<16.0 (-)	Cosgrove (1971)
<i>Serpentes (var)</i>	250	30	0/0.1 + 3	0.9	3.50 (90)	Cosgrove (1965)
<i>Coluber constrictor</i>	250	30	0/0.1 + 3	1.3	3.50 (90)	Cosgrove (1971)
<b>Testudines</b>						
<i>Terrapene carolina</i>	250	30	0/0.1 + 3	1.2	8.50 (120)	Cosgrove (1965)
	200	20	0.1/0	0.4	80.0 (30)	Altland, Highman & Wood (1951)
	200	20	0.1/0	0.4	12.5 (120)	Altland, Highman & Wood (1951)
	200	20	0.1/0	0.4	>5.00 (-)	Altland, Highman & Wood (1951)
<i>Terrapene carolina</i>	250	30	0/0.1 + 3	0.4	10.3 (120)	Cosgrove (1971)
<i>Chelydra serpentina</i>	300	20	0/0.1 + 3	1.2	10.0 (120)	Cosgrove (1971)
<i>Chrysemys picta</i>	300	20	0/0.1 + 3	0.9	<10.0 (120)	Cosgrove (1971)
<b>Crocodylia</b>						
<i>Alligator mississippiensis</i>	250	na	0.5/1	5.0	9.50 (60)	Bair, Park & Clarke (1968)
<b>Anura</b>						
<i>Bufo hemiophrys</i>	Ce-137			0.3	22.0 (30)	Tester, Ewert & Siniff (1970)
	Ce-137			0.3	22.0 (60)	Tester, Ewert & Siniff (1970)
<i>Bufo woodhousei fowleri</i>	Co-60			4.9	23.3 (30)	Landreth, Dunaway & Cosgrove (1974)
	Co-60			4.9	17.8 (50)	Landreth, Dunaway & Cosgrove (1974)
<i>Bufo melanostictus</i>	80	9	0.3/0	0.5	10.8 (30)	Guha & De (1974)
	80	9	0.3/0	0.5	8.00 (40)	Guha & De (1974)
<i>Rana pipiens</i>	200	15	0.5/0	0.5	7.00 (42)	Stearner (1950)
	250	15	1/0.5	1.3	7.55 (150)	Conger & Clinton (1973)
<i>Hyla squirella</i>	300	20	0.5/1	2.3	11.3 (50)	Conger & Clinton (1973)
<i>Hyla septentrionalis</i>	300	20	0.5/1	2.3	>15.0 (180)	Conger & Clinton (1973)
<i>Limnodynastes tasmaniensis</i>	Co-60			0.3	18.7 (160)	Panter (1986)
<i>Xenopus laevis</i>	Co-60			0.8	120 (30)	DiVita & Barr (1963)
	Co-60			0.8	20.0 (60)	DiVita & Barr (1963)
<b>Caudata</b>						
<i>Diemictylus viridescens</i>	250	30	0.5/1	1.5	14.9 (30)	Jakowska, Nigrelli & Sparrow (1958)
<i>Notophthalmus viridescens</i>	250	15	1/0.5	1.3	4.75 (150)	Conger & Clinton (1973)
<i>Amphiuma means</i>	250	30	0.5/1	0.8	32.8 (30)	Sparrow <i>et al.</i> (1970)
<i>Desmognathus fuscus</i>	250	30	0.5/1	0.7	9.70 (30)	Sparrow <i>et al.</i> (1970)
<i>Taricha granulosa</i>	300	20	2/0	0.4	24.7 (30)	Sparrow <i>et al.</i> (1970)
	100	na	0/0	2.6	30.0 (60)	Algard, Friedmann & McCurdy (1974)
<i>Necturus maculosus</i>	300	20	0.5/1	2.3	<2.15 (180)	Conger & Clinton (1973)
	250	30	0.5/1	0.8	35.5 (30)	Sparrow <i>et al.</i> (1970)

**Table 3.** Comparison of the most recent *in vivo* micro-CT studies. The most important parameters of the respective scanning protocols, as well as spatial resolution, scanning time, radiation dose and use of filters are indicated. A review of earlier studies can be found in Carlson *et al.* (2007)

References	Voltage (kV)	Al filter (mm)	Resolution ( $\mu$ m)	Time (min)	Radiation dose (Gy)	Dose rate (Gy min <sup>-1</sup> )
Willekens <i>et al.</i> (2010)	50	0.5	83	2.0	0.40	0.20
Vande Velde <i>et al.</i> (2015)	50	0.5	35	12.0	0.96	0.08
Laperre <i>et al.</i> (2011)	50	1.0	9	12.0	0.43	0.04
Laperre <i>et al.</i> (2011)	50	1.0	18	5.0	0.17	0.03
Detombe <i>et al.</i> (2013)	80	0	150	0.8	0.28	0.34
Foster & Ford (2010)	80	0.15	150	0.8	0.30	0.36
Foster & Ford (2010)	80	0.15	150	0.5	0.18	0.36
Foster & Ford (2010)	80	0.15	150	0.1	0.07	0.53
Figuroa <i>et al.</i> (2008)	80	0.5	45	2.4	0.07	0.03
Rodt <i>et al.</i> (2011)	80	1.8	47	18.1	0.23	0.01
Rodt <i>et al.</i> (2011)	80	1.8	94	10.0	0.15	0.02
Rodt <i>et al.</i> (2011)	80	1.8	94	10.0	0.13	0.01
Rodt <i>et al.</i> (2011)	80	1.8	94	22.0	0.15	0.01
Carlson <i>et al.</i> (2007)	80	1.0	156	1.0	0.02	0.02

1963). However, it must be noted that this effect might be partially diminished by the increased radiosensitivity due to higher oxygen tension at lower temperatures (Belli & Bonte 1963). Furthermore, survival appears to be higher in animals held at low ambient temperatures following irradiation (Patt & Swift 1948; O'Brien & Gojmerac 1956; Turner *et al.* 1967). In this case, however, it has been suggested that survival is prolonged because of a temporary delay in radiation damage manifestation (Berry & Oliver 1964). Hyperthermia, on the contrary, appears to directly enhance the radiation response (Ben-Hur, Elkind & Bronk 1974). Secondly, higher radiation dose rates (i.e. Gy min<sup>-1</sup>) might significantly increase radiosensitivity (Vogel, Clark & Jordan 1957; Neal 1960; Egami & Hama 1975). The radiation dose rate of recent *in vivo*  $\mu$ CT studies ranges from 0.01 to 0.53 Gy min<sup>-1</sup> (Table 3), while those used in studies assessing radiosensitivity in reptiles and amphibians (Table 2) are tenfold higher than the average  $\mu$ CT radiation dose rate.

#### EFFECTS OF SCANNING PARAMETERS ON RADIATION DOSE AND IMAGE QUALITY

The results from our radiation dose experiments reveal that three scanning parameters have a significant effect on radiation dose, image quality or both: tube voltage, distance to X-ray source and Cu filtration. The effects of these parameters are discussed in detail below.

##### Tube voltage

The tube voltage of current *in vivo*  $\mu$ CT studies ranges from 50 to 80 kV (Table 3). Our results show that radiation dose can be greatly reduced by decreasing the tube voltage to 50 kV without significant loss of image quality (Bischoff *et al.* 2009; Fig. 2, Table 1). However, the presence of a carapace in testudines might reduce the radiation dose by 21% (Altland, Highman & Wood 1951; Cosgrove 1965). Similarly, several lizard species, including *O. cataphractus*, possess osteoderms in the dermis, which could reduce the

tissue dose (Brooks 1962). A slightly higher tube voltage is to be considered (e.g. 85 kV), especially in reptiles that possess some form of dermal armour, to maintain high image quality of internal structures.

##### Distance to source

The main advantage of a rotating sample design is that the distance between the sample and X-ray source can be easily adjusted to obtain higher or lower spatial resolution. However, radiation dose increases exponentially with decreasing distance to the X-ray source (Fig. 4). Our experiments show that the radiation dose increased from 0.002 Gy min<sup>-1</sup> at 300 mm to 0.17 Gy min<sup>-1</sup> at 105 mm (Table 1). The distance to source depends on (i) the resolution required and (ii) the size of the animal. Scanning with low resolution relative to the actual structure size might cause an overestimation of object due to partial-volume effects (Bouxein *et al.* 2010). Hence, the distance to source should be reduced to obtain high precision measurements of small anatomical structures (e.g. osteoderms), especially in smaller animals. It is worthwhile to note that the resolution of  $\mu$ CT scans is affected by the size and resolution of the X-ray detector: by considering  $\mu$ CT scanners with larger, higher-resolution detectors, an increase in spatial resolution could be achieved while keeping the sample at the same distance from the X-ray source.

##### Cu filtration

Radiation exposure during  $\mu$ CT scanning can be reduced by making use of metal filtration (Rodt *et al.* 2011; Fig. 2, Table 1). The addition of a thicker Cu filter (i.e. 0.5 or 1.0 mm) in our study increased the noise and, consequently, decreased the image quality considerably (Fig. 2, Table 1). Cu filtration might therefore not be optimal because it results in less image contrast compared to, for example, Al filtration (Chakera *et al.* 1982). Nevertheless, while the addition of Cu filtration might not significantly

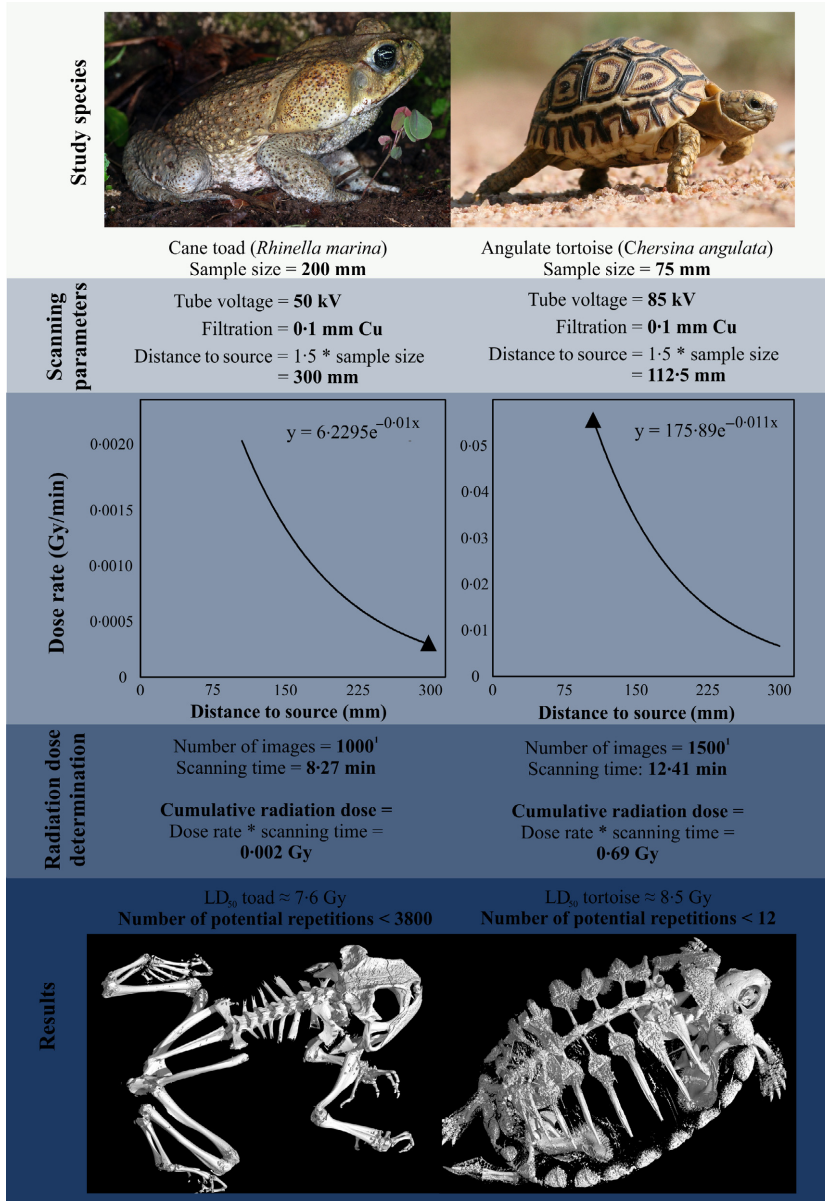


**Fig. 4.** Diagram illustrating two potential applications of the proposed *in vivo* micro-CT ( $\mu$ CT) scanning protocol and associated scan settings. The size of the sample determines the optimal distance to source (based on a  $2048 \times 2048$  pixel X-ray detector). These values can be used to calculate the cumulative radiation dose, which, in turn, determines the number of potential repetitions. <sup>1</sup>Tube voltage: tube voltage could be increased if the presence of osteoderms or a carapace is expected to affect the quality of internal structures. <sup>2</sup>Number of images: a higher number of images, especially in wide study objects, decrease the risk of artefacts. <sup>3</sup>LD<sub>50</sub>: lethal dose based on values presented in Table 3. See text for a detailed description. Cane toad: © Jason Mintzer/Shutterstock; Angulate tortoise: © JI de Wet/Shutterstock.

reduce the cumulative radiation dose, it filters out the low-energy photons that increase the risk of radiation-based symptoms (Kohn, Gooch & Keller 1988). Furthermore, filtering out the low-energy photons holds several imaging benefits including reduced scattering and beam hardening (Meganck *et al.* 2009).

TOWARDS A GENERAL FRAMEWORK FOR *IN VIVO*  $\mu$ CT SCANNING IN REPTILES AND AMPHIBIANS

The purpose of the study was to develop a protocol that can be adjusted to suit specific needs of researchers. We recommend that the following steps be taken during experimental design:

**1** Study animals should be exposed to the least possible amount of irradiation and scanning parameters must be set accordingly. Low tube voltage and metal filtration

should be used at all times. A slightly higher tube voltage, however, is warranted if shielding by carapace or osteoderms is expected to influence the image quality of internal structures. Using these settings, the cumulative radiation dose can be calculated for a study object of known size (Fig. 4).

**2** The dose measurements described in this protocol can be used as a reference guide, but it must be kept in mind that each X-ray source has different emission characteristics and therefore each system should require its own dose measurements. Hence, we suggest that preliminary radiation dose experiments should be conducted (e.g. by using an inexpensive commercial dosimeter) prior to the development of any experimental design to assure that similar values are obtained as those suggested in this protocol.

**3** We propose that the LD<sub>50</sub> recorded over the longest time period is used as proxy for radiosensitivity and that the

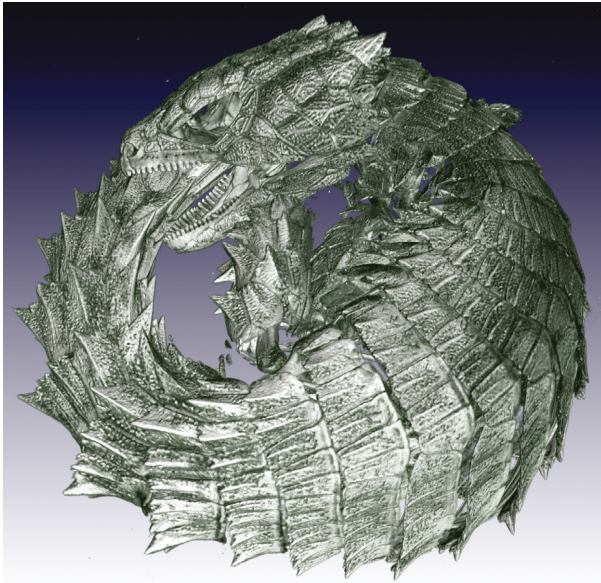


**Fig. 5.** 3D rendering of a live Armadillo lizard displaying defensive tail-biting behaviour. The specific animal entered defensive mode prior to the cooling stage and maintained this behaviour throughout the entire cooling and scanning period. The image was obtained by making use of the *in vivo* micro-CT ( $\mu$ CT) scanning protocol developed in this study. The image shows the organization of osteoderms embedded in the skin after digitally removing the scales.

radiation dose during  $\mu$ CT scanning (or cumulative dose in case of a longitudinal study) should lie below this upper limit. Thus, based on Table 2, the upper limit is 3.5 Gy [based on  $LD_{50(90)}$ ] for squamates, 8.5 Gy [based on  $LD_{50(120)}$ ] for testudines, 2.15 Gy [based on  $LD_{50(180)}$ ] for newts and 7.6 Gy [based on  $LD_{50(150)}$ ] for frogs. These values fall within the  $LD_{50(30)}$  range observed in various mammals (i.e. 2.5–10.5 Gy; see table 6.2 in Stabin 2007). Based on the total cumulative radiation dose and the  $LD_{50}$ , one can easily determine the number of potential repetitions. If more repetitions or higher image quality is required, parameters can be adjusted accordingly (see Fig. 2, Table 1).

**4** If the experimental design allows, we suggest that a recovery period should be implemented, either following a once-off scan or between consecutive scans. Ambient temperature should be kept low to avoid hyperthermia, which could enhance the radiation response (Ben-Hur, Elkind & Bronk 1974). In addition, close monitoring of blood counts is recommended to provide an early assessment of radiation exposure (Blakely *et al.* 2007).

Steps 1–3 are summarized in a diagram in Fig. 4 conceptualizing how the *in vivo*  $\mu$ CT protocol can be applied within ecological and evolutionary research. In the first example, researchers might want to investigate the effects of various control methods on growth and allometry in the invasive Cane toad, *Rhinella marina* (e.g. Beaty & Salice 2013). In the second example, researchers might want to provide more insight into the development of the carapace in the Angulate tortoise, *Chersina angulate* (e.g. Rice *et al.* 2016).

## CONCLUSION AND POTENTIAL APPLICATIONS

The proposed *in vivo*  $\mu$ CT scanning protocol offers ecologists and evolutionary biologists several benefits: (i) the low cumulative radiation doses allow for longitudinal studies and repetitive measurements of anatomical features (e.g. bones) when high spatial resolution is not required, thus conferring a huge advantage over *post-mortem* studies; (ii) smaller structures (e.g. osteoderms) can be easily examined in detail at high resolution without necessitating sacrifice of study subjects and supplement or replace time-consuming histological analyses; and (iii) in the absence of anaesthetics,  $\mu$ CT can be used to investigate temperature-independent behaviours displayed by organisms *in vivo*. For example, *O. cataphractus* deploys a defensive tail-biting strategy when threatened by a predator (Broeckhoven, Diedericks & Mouton 2015). *In vivo*  $\mu$ CT allowed us to obtain a high-resolution scan of this unique behaviour (Fig. 5, Video S2) which, combined with analytical software (e.g. finite element analysis), could provide novel information on how defensive morphologies are adapted to withstand deformations under a predatory attack. While the biomedical studies that employ *in vivo*  $\mu$ CT technology are advancing rapidly, future studies should focus on improving techniques and protocols that make use of commercial systems that are becoming widely available to ecologists and evolutionary biologists and address some of the practical limitations and challenges raised here.

## Acknowledgements

We would like to thank G. Diedericks for her assistance with collecting the lizard specimens. We are grateful to three anonymous reviewers for valuable comments on earlier versions of the manuscript. This research was supported by National Research Foundation (NRF) incentive funding to PLFN. CH is supported by an NRF South Africa Grant (81825 & 76912) and the Australian Research Council (Discovery Project DP150103017).

## Data accessibility

The data used to calculate image quality have been archived on Dryad Digital Repository <http://dx.doi.org/10.5061/dryad.pv6jlf> (Broeckhoven *et al.* 2016b).

## References

- Algard, F.T., Friedmann, G.B. & McCurdy, H.M. (1974) Responses of adult newts (Amphibia: Urodele) to x rays. *Canadian Journal of Zoology*, **52**, 665–669.
- Altland, P.D., Highman, B. & Wood, B. (1951) Some effects of x-radiation on turtle. *Journal of Experimental Zoology*, **118**, 1–193.
- Bair, W.J., Park, J.F. & Clarke, W.J. (1968) The radiosensitivity of alligators. *US Atomic Energy Commission, BNWL-714*, 1–18.
- Bartholomew, G.A. & Lasiewski, R.C. (1965) Heating and cooling rates, heart rate and simulated diving in the Galapagos marine iguana. *Comparative Biochemistry and Physiology*, **16**, 573–582.
- Bartholomew, G.A. & Tucker, V.A. (1964) Size, body temperature, thermal conductance, oxygen consumption, and heart rate in Australian varanid lizards. *Physiological Zoology*, **37**, 341–354.
- Bartholomew, G.A., Tucker, V.A. & Lee, A.K. (1965) Oxygen consumption, thermal conductance, and heart rate in the Australian skink *Tiliqua scincoides*. *Copeia*, **1965**, 169–173.
- Bauder, J.A.S., Handschuh, S., Metscher, B.D. & Krenn, H.W. (2013) Functional morphology of the feeding apparatus and evolution of proboscis length in metalmark butterflies (Lepidoptera: Riodinidae). *Biological Journal of the Linnean Society*, **110**, 291–304.

- Beaty, L.E. & Salice, C.J. (2013) Size matters: insights from an allometric approach to evaluate control methods for invasive Australian *Rhinella marina*. *Ecological Applications*, **23**, 1544–1553.
- Beck, A., Woods, S., Lansdowne, J.L. & Arens, D. (2013) The effects of multiple high-resolution peripheral quantitative computed tomography scans on bone healing in a rabbit radial bone defect model. *Bone*, **56**, 312–319.
- Belli, J.A. & Bonte, F.J. (1963) Influence of temperature on the radiation response of mammalian cells in tissue culture. *Radiation Research*, **18**, 272–276.
- Ben-Hur, E., Elkind, M.M. & Bronk, B.V. (1974) Thermally enhanced radioreponse of cultured Chinese hamster cells: inhibition of repair of sublethal damage and enhancement of lethal damage. *Radiation Research*, **58**, 38–51.
- Bennett, R.A. (1991) A review of anesthesia and chemical restraint in reptiles. *Journal of Zoo and Wildlife Medicine*, **22**, 282–303.
- Berry, R.J. & Oliver, R. (1964) Effect of post-irradiation incubation conditions on recovery between fractionated doses of X-rays. *Nature*, **201**, 94–96.
- Bertelsen, M.F., Mosley, C., Crawshaw, G.J., Dyson, D. & Smith, D.A. (2005) Inhalation anesthesia in Dumeril's monitor (*Varanus dumerilii*) with isoflurane, sevoflurane, and nitrous oxide: effects of inspired gases on induction and recovery. *Journal of Zoo and Wildlife Medicine*, **36**, 62–68.
- Bischoff, B., Hein, F., Meyer, T., Hadamitzky, M., Martinoff, S., Schömig, A. & Hausleiter, J. (2009) Trends in radiation protection in CT: present and future status. *Journal of Cardiovascular Computed Tomography*, **3**, 65–73.
- Blakely, W.F., Ossetrova, N.I., Manglapus, G.L., Salter, C.A., Levine, I.H., Jackson, W.E. et al. (2007) Amylase and blood cell-count hematological radiation-injury biomarkers in a rhesus monkey radiation model – use of multiparameter and integrated biological dosimetry. *Radiation Measurements*, **42**, 1164–1170.
- Boone, J.M., Velazquez, O. & Cherry, S.R. (2004) Small-animal X-ray dose from micro-CT. *Molecular Imaging*, **3**, 149–158.
- Bouxein, M.L., Boyd, S.K., Christiansen, B.A., Guldberg, R.E., Jepsen, K.J. & Müller, R. (2010) Guidelines for assessment of bone microstructure in rodents using micro-computed tomography. *Journal of Bone and Mineral Research*, **25**, 1468–1486.
- Boyd, S.K., Davison, P., Müller, R. & Gasser, J.A. (2006) Monitoring individual morphological changes over time in ovariectomized rats by in vivo micro-computed tomography. *Bone*, **39**, 854–862.
- Broeckhoven, C., Diedericks, G. & Mouton, P.L.F.N. (2015) What doesn't kill you might make you stronger: functional basis for variation in body armour. *Journal of Animal Ecology*, **84**, 1213–1221.
- Broeckhoven, C. & Mouton, P.L.F.N. (2015) Some like it hot: camera traps unravel the effects of weather conditions and predator presence on the activity levels of two lizards. *PLoS ONE*, **10**, e0137428.
- Broeckhoven, C., Diedericks, G., Hui, C., Makhubo, B.G. & Mouton, P.L.F.N. (2016a) Enemy at the gates: rapid defensive trait diversification in an adaptive radiation of lizards. *Evolution*, (in press), doi:10.1111/evo.13062
- Broeckhoven, C., du Plessis, A., le Roux, S.G., Mouton, P.L.F.N. & Hui, C. (2016b) Beauty is more than skin deep: a non-invasive protocol for in vivo anatomical study using micro-CT. *Dryad Digital Repository*, <http://dx.doi.org/10.5061/dryad.pv6j1f>
- Brooks, G.R. (1962) Resistance of the ground skink, *Lygosoma laterale*, to gamma radiation. *Herpetologica*, **18**, 128–129.
- Brouwers, J.E., Van Rietbergen, B. & Huiskes, R. (2007) No effects of in vivo micro-CT radiation on structural parameters and bone marrow cells in proximal tibia of wistar rats detected after eight weekly scans. *Journal of Orthopaedic Research*, **25**, 1325–1332.
- Brunst, V.V. (1958) The effect of total-body x-irradiation on the adult axolotl (*Siredon mexicanum*). *Radiation Research*, **8**, 32–45.
- Campbell, G.M. & Sophocleous, A. (2014) Quantitative analysis of bone and soft tissue by micro-computed tomography: applications to *ex vivo* and *in vivo* studies. *BoneKey Reports*, **3**, 564.
- Carlson, S.K., Classic, K.L., Bender, C.E. & Russell, S.J. (2007) Small animal absorbed radiation dose from serial micro-computed tomography imaging. *Molecular Imaging and Biology*, **9**, 78–82.
- Chakera, T.M.H., Fleay, R.F., Henson, P.W. & Cole, S.M. (1982) Dose reduction in radiology using heavy metal foils. *The British Journal of Radiology*, **55**, 853–858.
- Claussen, D.L. & Art, G.R. (1981) Heating and cooling rates in *Anolis carolinensis* and comparisons with other lizards. *Comparative Biochemistry and Physiology. Part A, Physiology*, **69**, 23–29.
- Conger, A.D. & Clinton, J.H. (1973) Nuclear volumes, DNA contents, and radiosensitivity in whole-body-irradiated amphibians. *Radiation Research*, **54**, 69–101.
- Cosgrove, G.E. (1965) The radiosensitivity of snakes and box turtles. *Radiation Research*, **25**, 706–712.
- Cosgrove, G.E. (1971) Reptilian radiography. *Journal of the American Veterinary Medical Association*, **159**, 1678–1684.
- Dana, S.W. & Tinkle, D.W. (1965) Effects of X-radiation on the testes of the lizard, *Uta stansburiana stejnegeri*. *International Journal of Radiation Biology and Related Studies in Physics, Chemistry, and Medicine*, **9**, 67–80.
- Detombe, S.A., Dunmore-Buyze, J., Petrov, I.E. & Drangova, M. (2013) X-ray dose delivered during a longitudinal micro-CT study has no adverse effect on cardiac and pulmonary tissue in C57BL/6 mice. *Acta Radiologica*, **54**, 435–441.
- DiVita, G. & Barr, A. (1963) Notes on the radiobiology of *Xenopus laevis*. *International Journal of Radiation Biology*, **6**, 485–486.
- Egami, N. & Hama, A. (1975) Dose-rate effects on the hatchability of irradiated embryos of the fish, *Oryzias latipes*. *International Journal of Radiation Biology and Related Studies in Physics, Chemistry, and Medicine*, **28**, 273–278.
- Elliott, J.C. & Dover, S.D. (1982) X-ray microtomography. *Journal of Microscopy*, **126**, 211–213.
- Feldkamp, L.A., Goldstein, S.A., Parfitt, M.A., Jesion, G. & Kleerekoper, M. (1989) The direct examination of three-dimensional bone architecture in vitro by computed tomography. *Journal of Bone and Mineral Research*, **4**, 3–11.
- Figueroa, S.D., Winkelmann, C.T., Miller, W.H., Volkert, W.A. & Hoffman, T.J. (2008) TLD assessment of mouse dosimetry during microCT imaging. *Medical Physics*, **35**, 3866–3874.
- Firbank, M.J., Coulthard, A., Harrison, R.M. & Williams, E.D. (1999) A comparison of two methods for measuring the signal to noise ratio on MR images. *Physics in Medicine and Biology*, **44**, N261–N264.
- Foster, W.K. & Ford, N.L. (2010) Investigating the effect of longitudinal micro-CT imaging on tumour growth in mice. *Physics in Medicine and Biology*, **56**, 315–326.
- Graves, E.E., Zhou, H., Chatterjee, R., Keall, P.J., Gambhir, S.S., Contag, C.H. & Boyer, A.L. (2007) Design and evaluation of a variable aperture collimator for conformal radiotherapy of small animals using a microCT scanner. *Medical Physics*, **34**, 4359–4367.
- Greenbaum, E., Stanley, E.L., Kusamba, C., Moninga, W.M., Goldberg, S.R. & Bursey, C.R. (2012) A new species of *Cordylus* (Squamata: Cordylidae) from the Marungu Plateau of south-eastern Democratic Republic of the Congo. *African Journal of Herpetology*, **61**, 14–39.
- Grigg, G.C. & Alchin, J. (1976) The role of the cardiovascular system in thermoregulation of *Crocodylus johnstoni*. *Physiological Zoology*, **49**, 24–36.
- Guha, T. & De, M.L. (1974) Mortality of the toad *Bufo melanostictus* after whole-body X-irradiation. *International Journal of Radiation Biology and Related Studies in Physics, Chemistry, and Medicine*, **26**, 77–80.
- Hoefler, A.M., Goodman, B.A. & Downes, S.J. (2003) Two effective and inexpensive methods for restraining small lizards. *Herpetological Review*, **34**, 223–224.
- Holdsworth, D.W. & Thornton, M.M. (2002) Micro-CT in small animal and specimen imaging. *Trends in Biotechnology*, **20**, 34–39.
- Jakowska, S., Nigrelli, R.F. & Sparrow, A.H. (1958) Radiobiology of the newt, *Diemictylus viridescens*. Hematological and histological effects of whole-body x-irradiation. *Zoologica*, **43**, 155–159.
- John-Alder, H.B., Morin, P.J. & Lawler, S. (1988) Thermal physiology, phenology, and distribution of tree frogs. *The American Naturalist*, **132**, 506–520.
- Kagadis, G.C., Loudos, G., Katsanos, K., Langer, S.G. & Nikiforidis, G.C. (2010) In vivo small animal imaging: current status and future prospects. *Medical Physics*, **37**, 6421–6442.
- Kinney, J.H., Lane, N.E. & Haupt, D.L. (1995) In vivo, three-dimensional microscopy of trabecular bone. *Journal of Bone and Mineral Research*, **10**, 264–270.
- Kleinbergs-Krisans, S. & Catlett, R.H. (1975) Radiosensitivity of the arenicolous lizard, *Uma notata*. *Radiation Research*, **61**, 110–117.
- Klinck, R.J., Campbell, G.M. & Boyd, S.K. (2008) Radiation effects on bone architecture in mice and rats resulting from in vivo micro-computed tomography scanning. *Medical Engineering & Physics*, **30**, 888–895.
- Kohn, M.L., Gooch, A.W. Jr & Keller, W.S. (1988) Filters for radiation reduction: a comparison. *Radiology*, **167**, 255–257.
- Kothari, R.M. & Patil, S.F. (1975) Effect of gamma irradiation on the common garden lizard, *Calotes versicolor* (Daud). *Journal of Herpetology*, **9**, 103–105.
- Kour, E.L. & Hutchison, V.H. (1970) Critical thermal tolerances and heating and cooling rates of lizards from diverse habitats. *Copeia*, **1970**, 219–229.
- Landreth, H.F., Dunaway, P.B. & Cosgrove, G.E. (1974) Effects of whole-body gamma irradiation on various life stages of the toad, *Bufo woodhousei fowleri*. *Radiation Research*, **58**, 432–438.
- Laperre, K., Depypere, M., van Gastel, N., Torrekens, S., Moermans, K., Bogaerts, R., Maes, F. & Carmeliet, G. (2011) Development of micro-CT protocols for in vivo follow-up of mouse bone architecture without major radiation side effects. *Bone*, **49**, 613–622.
- Lappenbusch, W.L. & Willis, D.L. (1970) The effect of dimethyl sulphoxide on the radiation response of the rough-skinned newt (*Taricha granulosa*).

- International Journal of Radiation Biology and Related Studies in Physics, Chemistry, and Medicine*, **18**, 217–233.
- Longley, L. (2008) *Anaesthesia of Exotic Pets*. Elsevier Saunders, Edinburgh, UK.
- Losos, J.B., Schoener, T.W. & Spiller, D.A. (2004) Predator-induced behaviour shifts and natural selection in field-experimental lizard populations. *Nature*, **432**, 505–508.
- Losos, J.B., Mouton, P.L.F.N., Bickel, R., Cornelius, I. & Ruddock, L. (2002) The effect of body armature on escape behaviour in cordylid lizards. *Animal Behaviour*, **64**, 313–321.
- Main, R.P., Lynch, M.E. & van der Meulen, M.C. (2010) *In vivo* tibial stiffness is maintained by whole bone morphology and cross-sectional geometry in growing female mice. *Journal of Biomechanics*, **43**, 2689–2694.
- McConnachie, S., Alexander, G.J. & Whiting, M.J. (2007) Lower temperature tolerance in the temperate, ambush foraging lizard *Pseudocordylus melanotus melanotus*. *Journal of Thermal Biology*, **32**, 66–71.
- Meganck, J.A., Kozloff, K.M., Thornton, M.M., Broski, S.M. & Goldstein, S.A. (2009) Beam hardening artifacts in micro-computed tomography scanning can be reduced by X-ray beam filtration and the resulting images can be used to accurately measure BMD. *Bone*, **45**, 1104–1116.
- Mosley, C.A. (2005) Anesthesia and analgesia in reptiles. *Seminars in Avian and Exotic Pet Medicine* (ed. G.R. Pettifer), pp. 243–262. WB Saunders, Philadelphia, PA, USA.
- Müller, J., Hipsley, C.A., Head, J.J., Kardjilov, N., Hilger, A., Wuttke, M. & Reisz, R.R. (2011) Eocene lizard from Germany reveals amphisbaenian origins. *Nature*, **473**, 364–367.
- Nagy, K.A. & Medica, P.A. (1985) Altered energy metabolism in an irradiated population of lizards at the Nevada Test Site. *Radiation Research*, **103**, 98–104.
- Neal, F.E. (1960) Variation of acute mortality with dose-rate in mice exposed to single large doses of whole-body X-radiation. *International Journal of Radiation Biology and Related Studies in Physics, Chemistry, and Medicine*, **2**, 295–300.
- O'Brien, J.P. & Gojmerac, W.L. (1956) Radiosensitivity of larval and adult amphibia in relation to temperature during and subsequent to irradiation. *Experimental Biology and Medicine*, **92**, 13–16.
- O'Connor, P.M., Sertich, J.J., Stevens, N.J., Roberts, E.M., Gottfried, M.D., Hieronylus, T.L. *et al.* (2010) The evolution of mammal-like crocodyliforms in the Cretaceous Period of Gondwana. *Nature*, **466**, 748–751.
- Panter, H.C. (1986) Variations in radiosensitivity during development of the frog *Limnodynastes tasmaniensis*. *Journal of Experimental Zoology*, **238**, 193–199.
- Patt, H.M. & Swift, M.N. (1948) Influence of temperature on the response of frogs to X irradiation. *American Journal of Physiology*, **155**, 388–393.
- Pearson, A.K., Licht, P., Nagy, K.A. & Medica, P.A. (1978) Endocrine function and reproductive impairment in an irradiated population of the lizard *Uta stansburiana*. *Radiation Research*, **76**, 610–623.
- du Plessis, A., le Roux, S.G. & Guelpa, A. (2016) The CT Scanner Facility at Stellenbosch University: an open access X-ray computed tomography laboratory. *Nuclear Instruments and Methods in Physics Research Section B*, **384**, 42–490.
- Rice, R., Kallonen, A., Cebra-Thomas, J. & Gilbert, S.F. (2016) Development of the turtle plastron, the order-defining skeletal structure. *Proceedings of the National Academy of Sciences of the United States of America*, **113**, 5317–5322.
- Ritman, E.L. (2004) Micro-computed tomography – current status and developments. *Annual Review of Biomedical Engineering*, **6**, 185–208.
- Rodt, T., Luepke, M., Boehm, C., von Falck, C., Stamm, G., Borlak, J., Seifert, H. & Galanski, M. (2011) Phantom and cadaver measurements of dose and dose distribution in micro-CT of the chest in mice. *Acta Radiologica*, **52**, 75–80.
- Roushdy, H.M., Mazhar, F.M., Ashry, M.A. & Refaat, S.M. (1979) Changes in developmental stages of the Egyptian lizard *Chalcides ocellatus* due to different radiation exposures. *Arab Journal of Nuclear Sciences and Applications*, **12**, 495–507.
- Rüeggsegger, P., Koller, B. & Müller, R. (1996) A microtomographic system for the nondestructive evaluation of bone architecture. *Calcified Tissue International*, **58**, 24–29.
- Schambach, S.J., Bag, S., Schilling, L., Groden, C. & Brockmann, M.A. (2010) Application of micro-CT in small animal imaging. *Methods*, **50**, 2–13.
- Seidel, M.R. (1979) The osteoderms of the American alligator and their functional significance. *Herpetologica*, **35**, 375–380.
- Sherratt, E., del Rosario Castañeda, M., Garwood, R.J., Mahler, D.L., Sanger, T.J., Herrel, A., de Queiroz, K. & Losos, J.B. (2015) Amber fossils demonstrate deep-time stability of Caribbean lizard communities. *Proceedings of the National Academy of Sciences of the United States of America*, **112**, 9961–9966.
- Sladky, K.K. & Mans, C. (2012) Clinical anesthesia in reptiles. *Journal of Exotic Pet Medicine*, **21**, 17–31.
- Smith, E.N. (1976) Heating and cooling rates of the American alligator, *Alligator mississippiensis*. *Physiological Zoology*, **49**, 37–48.
- Sparrow, A.H., Nauman, C.H., Donnelly, G.M., Willis, D.L. & Baker, D.G. (1970) Radiosensitivities of selected amphibians in relation to their nuclear and chromosome volumes. *Radiation Research*, **42**, 353–371.
- Spray, D.C. & May, M.L. (1972) Heating and cooling rates in four species of turtles. *Comparative Biochemistry and Physiology. Part A, Physiology*, **41**, 507–522.
- Stabin, M.G. (2007) *Radiation Protection and Dosimetry: An Introduction to Health Physics*. Springer, New York, NY, USA.
- Stearner, P.S. (1950) The effects of x irradiation on *Rana pipiens* (leopard frog), with special reference to survival and to the response of the peripheral blood. *Journal of Experimental Zoology*, **115**, 251–262.
- Storer, J.B. & Hempelmann, L.H. (1952) Hypothermia and increased survival rate of infant mice irradiated with X-rays. *American Journal of Physiology*, **171**, 341–348.
- Sturbaum, B.A. (1982) Temperature regulation in turtles. *Comparative Biochemistry and Physiology. Part A, Physiology*, **72**, 615–620.
- Taschereau, R., Chow, P.L. & Chatzioannou, A.F. (2006) Monte Carlo simulations of dose from microCT imaging procedures in a realistic mouse phantom. *Medical Physics*, **33**, 216–224.
- Tester, J.R., Ewert, M.A. & Siniff, D.B. (1970) Effects of ionizing radiation on natural and laboratory populations of Manitoba toads, *Bufo hemiophysys*. *Radiation Research*, **44**, 379–389.
- Turner, F.B. & Medica, P.A. (1977) Sterility among female lizards (*Uta stansburiana*) exposed to continuous  $\gamma$  irradiation. *Radiation Research*, **70**, 154–163.
- Turner, F.B., Lannom, J.R., Kania, H.J. & Kowalewsky, B.W. (1967) Acute gamma irradiation experiments with the lizard *Uta stansburiana*. *Radiation Research*, **31**, 27–35.
- Vande Velde, G., De Langhe, E., Poelmans, J., Bruyndonckx, P., d'Agostino, E., Verbeken, E., Bogaerts, R., Lories, R. & Himmelreich, U. (2015) Longitudinal in vivo microcomputed tomography of mouse lungs: no evidence for radiotoxicity. *American Journal of Physiology. Lung Cellular and Molecular Physiology*, **309**, 271–279.
- Vogel, H.H. Jr, Clark, J.W. & Jordan, D.L. (1957) Comparative mortality following single whole-body exposures of mice to fission neutrons and Co60 gamma rays 1. *Radiology*, **68**, 386–398.
- Weathers, W.W. & White, F.N. (1971) Physiological thermoregulation in turtles. *American Journal of Physiology*, **221**, 704–710.
- Willekens, I., Buls, N., Lahoutte, T., Baeyens, L., Vanhove, C., Cavellers, V., Deklerck, R., Bossuyt, A. & de Mey, J. (2010) Evaluation of the radiation dose in micro-CT with optimization of the scan protocol. *Contrast Media & Molecular Imaging*, **5**, 201–207.
- Willis, D.L. & McCourry, M.M. (1968) Radiosensitivity of the western fence lizard (*Sceloporus occidentalis*) and the desert crested lizard (*Dipsosaurus dorsalis*). *Radiation Research*, **35**, 574.

Received 8 August 2016; accepted 15 September 2016

Handling Editor: Natalie Cooper

## Supporting Information

Additional Supporting Information may be found online in the supporting information tab for this article:

**Video S1.** Video showing a real-time *in vivo*  $\mu$ CT scan.

**Video S2.** Video showing a 3D rendering of tail-biting behaviour in the Armadillo lizard.